1975A&A....41..329Z

Astron. & Astrophys. 41, 329 – 344 (1975)

The Dynamical Tide in Close Binaries

J.-P. Zahn

Observatoire de Nice, and Joint Institute for Laboratory Astrophysics, University of Colorado, Boulder

Received February 24, 1975

Summary. The non-adiabatic oscillations of a star, driven by an outer rotating gravitational field, have been studied by the use of matched asymptotic expansions. The interior and envelope solutions in this procedure are derived in Sections 2 and 3. The results apply to stars which have a convective core and a radiative envelope, and they are discussed in Section 4.

We find that the resonances of the free gravity modes are damped by radiative dissipation, which operates in a relatively thin region below the surface of the star. Due to that dissipation, some properties of the dynamical tide have observable consequences in close binary systems: i) A torque is applied to a binary component; this serves to make it corotate with its companion in a time which can be short compared to its nuclear life. ii) Before that synchronization is achieved, the brightness distribution over the surface of the star is in general phase shifted relative to the external driving potential.

Key words: stellar structure — non-radial oscillations — close binaries

1. Introduction

Most studies of the internal structure of stars deformed by the gravitational field of a close companion have implicitly assumed that such stars are at all times in hydrostatic equilibrium. This treatment is justified when the binary component rotates uniformly in perfect synchronism with a circular orbital motion, and its tidal bulges are steady in time. If this condition is not fulfilled, the star senses a variable external gravitational field and becomes liable to oscillatory motions which are representable as both an equilibrium and a dynamical tide. The former is again just the instantaneous shape obtained by balancing the pressure and gravity forces.

Cowling (1941) was the first to describe such forced oscillations of a star, but he restricted his attention to the possible resonances of the lowest order gravity modes. We extended his work to the much higher overtones which are likely to be excited in close binaries (Zahn, 1970; hereafter referred to as Paper I). In contrast with Cowling, we found that it was not necessary to come very close to a resonance with a free mode of oscillation in order to achieve tides with large surface amplitudes. But this result was questionable since we, like Cowling, used the adiabatic approximation; near the surface of a star, where we predicted the large amplitudes, this approximation becomes very poor, and especially so for the long periods of interest. We have therefore returned to this problem, and will here take into account the effects of radiative damping.

But our principal motivation in undertaking this study is to pursue our search for physical mechanisms capable of synchronizing the rotation of close binary stars with their orbital motion, as is generally observed. To achieve this result, a torque must be applied to the stars, which requires the tidal deformation to be phase shifted with respect to the external potential. Various dissipative processes may be responsible for such a phase shift, but only a detailed analysis will reveal if they are efficient enough to produce the anticipated results. In a previous investigation dealing with only the equilibrium tide, we found that this tide, when damped by turbulent viscosity in a stellar convection zone, creates a torque which is strong enough to explain some dynamical properties of late-type close binaries, such as the negligible eccentricity of their orbits (Zahn, 1966). However, this viscous mechanism is efficient only in stars with a large outer convection zone; the torque predicted for stars lacking such a convective envelope is too weak to account for the observed synchronism in close binaries whose spectral type is earlier than *F* (Plavec, 1970).

This leads us to examine whether the dynamical tide, damped by radiative dissipation, might not be of greater efficiency. The aim of the present article is to include the effects of radiative damping in the description of the forced oscillations of a star possessing a convective core and a radiative envelope. We will do so in the simplest possible manner: since the adiabatic approximation fails only in a relatively shallow region below the surface, this region will be treated just as a boundary layer of polytropic structure. The star will thus be

© European Southern Observatory • Provided by the NASA Astrophysics Data System

1975A&A....41..329Z

divided in two domains: the adiabatic interior and the non-adiabatic envelope. Matched asymptotic expansions will be used, as in Paper I, to determine the functions describing the forced oscillation in these two regions.

As in Paper I, we will again completely ignore the rotation of the stars, though some hazards exist in doing so. For instance, one knows that the Coriolis force alters the non-radial modes which are excited by the outer potential (Cowling and Newing, 1949; Ledoux, 1951). Moreover, in the presence of rotation new modes will appear, and these may well contribute to the forced oscillation; such modes are related to the Rossby waves and they have a strong toroidal component.

We previously examined the effect of rotation on the equilibrium tide and found that the Coriolis force produces a toroidal velocity field, in addition to the purely poloidal field for no rotation (Zahn, 1966). The behavior of this toroidal field is particularly striking in a star which is strictly in uniform rotation: for some values of the rotational velocity, such a star undergoes what we called a pseudo-resonance, in which the toroidal component attains very large amplitudes. But this phenomenon requires the rather peculiar condition of solid body rotation, which is not likely to be achieved before the rotation of the star is fully synchronized with the orbital motion. For the more general case where there is at least some differential rotation present with depth, we found that the toroidal component of the equilibrium tide contributes only moderately to the torque which is applied to the star. We hope that the latter weak influence will also be true for the dynamical tide, and that the inclusion of rotational effects would not qualitatively change the results to be derived here.

2. The Oscillation in the Adiabatic Interior

We will first determine the functions which describe the forced oscillation in the deep interior of the star, where its behavior is nearly adiabatic. In this section, we will often refer to equations or results already derived in Paper I; the Roman I will identify the expressions quoted from that article. We will retain the notation that ϱ, P and T represent the unperturbed density, pressure and temperature. Further, the displacement field, and the Eulerian perturbations of both the pressure and the total gravitational potential, are again expanded in spherical harmonics as

$$\boldsymbol{\delta r}=\mathrm{Re}\left[a(r)Y_n^m(\theta,\phi,t)\,,\, b(r)\frac{dY_n^m}{d\theta}\,,\, -imb(r)\frac{Y_n^m}{\sin\theta}\right], \tag{2.1}$$

$$\delta P=\varrho(r)\mathrm{Re}[(\chi(r)-\Phi(r))Y_n^m(\theta,\phi,t)]\,, \tag{2.2}$$

$$\delta V=\mathrm{Re}[\Psi(r)Y_n^m(\theta,\phi,t)]\,, \tag{2.3}$$

where

$$Y_n^m(\theta,\phi,t)=P_n^m(\cos\theta)\exp i(\sigma t-m\phi)\,, \tag{2.4}$$

and a, b, χ, Φ and Ψ are functions of just the radial coordinate r (to simplify the notation, we shall omit their indices m and n).

As in Paper I, the oscillation will be driven by a single component of the outer harmonic potential, expressed as

$$U(r,\theta,\phi)\exp i\sigma t=U_n^m(r/R)^nY_n^m(\theta,\phi,t)\,. \tag{2.5}$$

and thus rotating with the phase velocity σ/m. The total perturbed potential is the sum of that outer potential and of the inner potential created by the perturbed mass configuration, so that

$$\Psi(r)=U_n^m(r/R)^n+\Phi(r)\,. \tag{2.6}$$

The functions a, χ and Ψ are determined by the fourth-order differential system [cf. (I; 2a–2e)]

$$\frac{d}{dr}(r^2a)=\frac{\varrho r^2}{\Gamma P}(ga+\Psi-\chi)+\frac{n(n+1)}{\sigma^2}\chi\,, \tag{2.7}$$

$$\frac{d\chi}{dr}=(\sigma^2+gA)a-A(\chi-\Psi)\,, \tag{2.8}$$

$$\frac{d}{dr}\left(r^2\frac{d\Psi}{dr}\right)-n(n+1)\Psi=4\pi G\varrho r^2\tilde{\varrho} \tag{2.9a}$$

with

$$\frac{\tilde{\varrho}}{\varrho}=\frac{\varrho}{\Gamma P}(\chi-\psi)-Aa\,. \tag{2.9b}$$

The boundary conditions which must be satisfied by the solutions are

$$a=\chi=\Psi=0 \quad \text{at the center} \quad (r=0)\,, \tag{2.10}$$

and

$$\left.\begin{aligned} &ga+\Psi-\chi=0\\ &r\frac{d\Psi}{dr}+(n+1)\Psi=(2n+1)U_n^m \end{aligned}\right\} \text{ at the surface } (r=R)\,. \tag{2.11}$$

Here again the function A measures the difference between the actual density gradient and the adiabatic one, namely

$$A=\frac{d}{dr}\ln\varrho-\frac{1}{\Gamma}\frac{d}{dr}\ln P\,; \tag{2.12}$$

its product with the local gravity, $-gA$, is the square of the Brunt-Väisälä frequency.

These equations will be solved in the limiting case where the excitation frequency σ is small compared to the frequency associated with the free fall time, i.e. $\sigma^2R/g_s\ll 1$, with g_s being the surface gravity GM/R^2. Also, it is convenient to use hereafter the fractional radius $x=r/R$ as the independent variable.

© European Southern Observatory • Provided by the NASA Astrophysics Data System

1975A&A....41..329Z

a) Solution in the Convective Core

In the convective core, where $A=0$, the elimination of χ between Eqs. (2.7) and (2.8) leads to a second-order differential equation for the function $X=\varrho x^2 a(x)$, namely

$$\mathscr{L}(X)=\varrho z' , \tag{2.13}$$

where the differential operator is

$$\mathscr{L}(X)=X''-(\varrho'/\varrho)X'-n(n+1)X/x^2 , \tag{2.14a}$$

and a prime indicates a derivative with respect to x. The function $z(x)$ on the right-hand side is related to the perturbed potential by

$$z=-(x^2\varrho'/g\varrho)\Psi . \tag{2.14b}$$

[To simplify this Eq. (2.13), we used the property that $\sigma^2\varrho r^2/\Gamma P \ll 1$.]

We can formally express the general solution of Eq. (2.13) in terms of the two independent solutions X_1, X_2 of its homogeneous counterpart $\mathscr{L}(X)=0$ as

$$\varrho x^2 a=X_1[C-\textstyle\int_0^x \Lambda^{-1}\varrho z' X_2 dx]+X_2\int_0^x \Lambda^{-1}\varrho z' X_1 dx . \tag{2.15}$$

We have chosen X_1 as the solution which is regular at the center $x=0$; C is an undetermined integration constant and Λ is the Wronskian

$$\Lambda=X_1X_2'-X_2X_1'=\mathrm{cst}\cdot\varrho . \tag{2.16}$$

Re-expressed in terms of the original function a, the solution in the convective core becomes

$$a=a_1[C-\textstyle\int_0^x \Lambda^{-1}\varrho z' X_2 dx]+a_2\int_0^x \Lambda^{-1}\varrho z' X_1 dx \tag{2.17}$$

where $a_1=X_1(\varrho x^2)^{-1}$ and similarly $a_2=X_2(\varrho x^2)^{-1}$. It can be easily verified that a_1 is also regular at the center.

b) Solution in the Radiative Zone

In the radiative region above the convective core, where now $A<0$, the elimination of χ between Eqs. (2.7) and (2.8) again leads to a second-order equation, which was given in Paper I (I; 17). To the lowest order in $\sigma^2 R/g_s$, this equation reduces to

$$a''+a'\frac{d}{dx}\ln(\varrho x^2)-\frac{n(n+1)gA}{\sigma^2x^2}a=\frac{n(n+1)A}{\sigma^2x^2}\Psi . \tag{2.18}$$

This equation can be simplified by taking instead of a the new function

$$W=\left(\frac{d\eta}{dx}\right)^{1/2}\varrho^{1/2}x^2 a \tag{2.19}$$

and introducing the independent variable η, defined in Paper I as

$$\frac{2}{3}v\eta^{3/2}=\int_{x_f}^x\left[\frac{-n(n+1)gA}{\sigma^2x^2}\right]^{1/2}dx=\tau_c , \tag{2.20}$$

where the large parameter v is chosen so that $d\eta/dx=1$ for $\eta=0$ (that is at the boundary of the convective core $x=x_f$). With these transformations, the differential equation (2.18) assumes the simpler form

$$\frac{d^2W}{d\eta^2}+v^2\eta W=v^2\eta Z , \tag{2.21}$$

where

$$Z=-\left(\frac{d\eta}{dx}\right)^{1/2}\varrho^{1/2}x^2\frac{\Psi}{g} . \tag{2.22}$$

We can again express the general solution of this inhomogeneous equation in terms of two independent solutions of its homogeneous counterpart as

$$W=W^\dagger+\left\{Z(\eta)-Z(0)\Gamma(2/3)\,(\tau_c/2)^{1/3}J_{-1/3}(\tau_c)-\left(\frac{dZ}{d\eta}\right)_{\eta=0}\Gamma(4/3)\,(v/3)^{-2/3}(\tau_c/2)^{1/3}J_{1/3}(\tau_c)\right\} . \tag{2.23}$$

This solution has been constructed so that the term in the brackets vanishes at $\eta=0$, as well as its derivative. $W^\dagger$ stands for the most general solution of the homogeneous equation.

Let us now match this solution to the solution valid in the convective core. For this purpose, it is convenient to return to the original function a, written as

$$a=C_1a_1+C_2a_2+\left[\left(\frac{d\eta}{dx}\right)^{1/2}\varrho^{1/2}x^2\right]^{1/2}\{----\} . \tag{2.24}$$

Here we have split the general solution of the homogeneous equation into its two components a_1 and a_2. These functions obey different equations in the convective core and in the radiative region, but are so chosen, in the latter domain, that they and their first derivatives are continuous at the boundary of the convective core ($x=x_f$, or $\eta=0$).

The matching of the function a itself, as expressed by Eq. (2.17) in the convective core and by Eq. (2.24) above in the radiative region, is achieved at $x=x_f$ by requiring

$$C_1\begin{pmatrix}a_1\\a_1'\end{pmatrix}+C_2\begin{pmatrix}a_2\\a_2'\end{pmatrix}=[C-\textstyle\int_0^{x_f}\Lambda^{-1}\varrho Z' X_2 dx]\begin{pmatrix}a_1\\a_1'\end{pmatrix}+[\int_0^{x_f}\Lambda^{-1}\varrho Z' X_1 dx]\begin{pmatrix}a_2\\a_2'\end{pmatrix} . \tag{2.25}$$

This determines one of the constants in (2.24), namely

$$C_2=\textstyle\int_0^{x_f}\Lambda^{-1}\varrho Z' X_1 dx ; \tag{2.26}$$

the other constant C_1 remains unknown, since it involves C which has not yet been specified. Introducing the Wronskian Λ_a relative to the solutions a_1 and a_2, we can transform the coefficient C_2 to become

$$C_2=\frac{a_1(x_f)}{x_f^2\Lambda_a(x_f)}\int_0^{x_f}\frac{X_1(x)}{X_1(x_f)}Z'(x)dx . \tag{2.27}$$

© European Southern Observatory • Provided by the NASA Astrophysics Data System

1975A&A....41..329Z

Since a_1 involves both Bessel functions $J_{1/3}$ and $J_{-1/3}$, as discussed in Paper I, we can take for a_2 the simple form

$$a_2 = \text{cst} \cdot \left(\frac{d\eta}{dx}\right)^{-1/2} \varrho^{-1/2} x^{-2} (\tau_c/2)^{1/3} J_{1/3}(\tau_c) \tag{2.28}$$

which is linearly independent from a_1. The product $C_2 a_2$ then becomes

$$C_2 a_2 = \Gamma(4/3)\,(v/3)^{-5/6} x_f^{-2} \int_0^{x_f} (X/X_f) z' dx \cdot \left[\frac{(\varrho x^4)_f}{\varrho x^4}\right]^{1/2} \left[\frac{(-gAx^{-2})'_f}{-gAx^{-2}}\right]^{1/4} (\tau_c/2)^{1/2} J_{1/3}(\tau_c), \tag{2.29}$$

where the subscript f denotes that a given function is evaluated at $x = x_f$. We will further write X_1 simply as X hereafter, since X_2 no longer appears.

c) Asymptotic Form and Matching with the Outer Solution

Sufficiently far from the convective core, where we can replace the Bessel functions by their asymptotic expressions for large τ_c, the solution for a can be written as

$$a = -\Psi/g + \varrho^{-1/2} x^{-2} (-gAx^{-2})^{-1/4} \cdot [(K_c + N_1)\cos(\tau_c - \pi/12) + (\alpha/\beta)(K_c + N_2)\cos(\tau_c - 5\pi/12)]. \tag{2.30}$$

K_c here replaces the undetermined constant C_1, and the coefficients N_1 and N_2 are given by

$$N_1 = \pi^{-1/2}\Gamma(2/3)\,(v/3)^{-1/6} \varrho_f^{1/2} [(-gAx^2)'_f]^{1/4} (\Psi/g)_f, \tag{2.31}$$

$$N_2 = \pi^{-1/2}\Gamma(4/3)\,(v/3)^{-5/6} (\beta/\alpha) \varrho_f^{1/2} [(-gAx^2)'_f]^{1/4} \cdot \left\{(\Psi/g)_f \left[\ln\left[\left(\frac{d\eta}{dx}\right)^{1/2} \varrho^{1/2} x^2 \frac{\Psi}{g}\right]\right]'_f + x_f^{-2} \int_0^{x_f} (X/X_f) z' dx\right\}. \tag{2.32}$$

The ratio α/β between the amplitudes of the Bessel functions $J_{1/3}$ and $J_{-1/3}$ is determined by the continuity condition which the homogeneous solution $C_1 a_2 + C_2 a_2$ must satisfy at the boundary of the convective core. Using there the function X instead of a, this condition can be written [cf. Eq. (I; 21)] as

$$\frac{\alpha}{\beta}\frac{\Gamma(2/3)}{\Gamma(4/3)}\left(\frac{v}{3}\right)^{2/3} = \left\{\ln\left[\left(\frac{d\eta}{dx}\right)^{1/2} \varrho^{-1/2} X\right]\right\}'_f. \tag{2.33}$$

As it is indicated in Eq. (2.30), the forced oscillation is composed of two distinct parts. The first term is readily identified as the equilibrium tide; its amplitude, which can be calculated simply by assuming that the star is in hydrostatic equilibrium, is given by $a_E = -\Psi/g$. The second term represents the dynamical tide; to determine it completely, we must first evaluate the constant K_c.

We can calculate K_c by matching the interior solution (2.30) with an envelope solution integrated inwards from the surface of the star, much as in Paper I. If the oscillation were adiabatic throughout the star, this envelope solution would have the asymptotic form of

$$a = -\Psi/g - K_s \varrho^{-1/2} x^{-2} (-gAx^{-2})^{-1/4} \sin(\tau_s - \pi/4 - \nu\pi/2) \tag{2.34}$$

where

$$\tau_s = \int_x^1 \left[\frac{-n(n+1)gA}{\sigma^2 x^2}\right]^{1/2} dx, \tag{2.35}$$

again to the lowest order in $\sigma^2 g_s/R$ and far enough from the surface [cf. (I; 24a)]. When we take radiative dissipation into account near the surface, it is as if the boundary, which functions as a perfect reflector in the adiabatic case, becomes partially absorbent. As a result, the oscillation acquires a travelling component (being only a stationary wave in the adiabatic case), so that in the adiabatic interior

$$a = -\Psi/g - K_s \varrho^{-1/2} x^{-2} (-gAx^{-2})^{-1/4} [\sin(\tau_s - \tau_0) + i\gamma\cos(\tau_s - \tau_0)]. \tag{2.36}$$

This is the most general form of the solution of Eq. (2.18) in the interior region situated far enough from both the surface and the convective core, in which the wavelength of the oscillation is small compared to the other characteristic scales of the problem. This form is an obvious generalization of (2.34); it can also be obtained directly by the WKB technique. Let us notice that the oscillatory function describing the dynamical tide in (2.36) is just the solution of the homogeneous form of Eq. (2.18); its amplitude, as measured by K_s, must thus be determined by matching this envelope solution with the interior solution (2.30).

In this expression (2.36), τ_0 is the phase extrapolated to the surface; the amplitude K_s is here complex. As we will see, γ plays the role of a damping constant; from its two possible determinations, we take that which is smaller than unity by a suitable choice of τ_0. There is unfortunately no analytical expression available for these parameters, and hence they must be determined by numerically integrating the non-adiabatic equations from the surface to some matching point. We will deal with this in Section 3; let us just assume here that these constants are all known, and thus proceed now to complete the matching of the interior and envelope solutions.

To achieve this matching, it is useful to introduce the argument ψ, which is a function of the frequently alone for a given model, as

$$\psi = \int_{x_f}^1 \left[\frac{-n(n+1)gA}{\sigma^2 x^2}\right]^{1/2} dx - \frac{\pi}{12} - \tau_0. \tag{2.37}$$

© European Southern Observatory • Provided by the NASA Astrophysics Data System

1975A&A....41..329Z

By comparing the asymptotic expressions of a given in Eqs. (2.30) and (2.36), we can express the matching condition as a relation between K_s and ψ, with

$$K_s = -\frac{\sqrt{3}}{2}\frac{\alpha}{\beta}\frac{N_1 - N_2}{\cos\psi - i\gamma\sin\psi} = \frac{-K_0}{\cos\psi - i\gamma\sin\psi}. \tag{2.38}$$

This expression has been slightly simplified, using the property that α/β is very small compared to unity. We can likewise evaluate the amplitude of the $J_{-1/3}$ term in (2.30) as

$$K_c + N_1 = K_0 \frac{\cos(\psi - \pi/3) - i\gamma\sin(\psi - \pi/3)}{\cos\psi - i\gamma\sin\psi}, \tag{2.39}$$

which will be of some use later on. After some lengthy but straightforward transformations, the coefficient K_0 can be written as

$$K_0 = \frac{\sqrt{3}\Gamma(4/3)}{2\sqrt{\pi}}\left(\frac{v}{3}\right)^{-5/6} \varrho_f^{1/2}\left[\left(\frac{-gA}{x^2}\right)'\right]^{1/4}\frac{U_n^m}{g_s} \cdot\left\{\frac{g_s}{U_n^m}\int_0^{x_f}\left[\left(\frac{x^2\Psi}{g}\right)'' - \frac{n(n+1)}{x^2}\left(\frac{x^2\Psi}{g}\right)\right]\frac{X}{X_f}dx\right\} \tag{2.40}$$

(again the subscript f denotes that a given expression is evaluated at the boundary of the convective core, $x = x_f$).

We can see from (2.38) that the amplitude of the dynamical tide, as measured by K_s, undergoes resonances for $\psi = \pi/2 + k\pi$, but the maximum amplitude is limited by the presence of the damping constant γ. In the dimensionless units of $s = (\sigma^2 R/g_s)^{1/2}$, the resonance frequencies are given by

$$s_k^{-1} = \frac{\Delta P}{\pi}\left(\psi + \frac{\pi}{12} + \tau_0\right) = \Delta P(k + k_0) \tag{2.41}$$

where

$$\Delta P = \pi\left[\frac{GM}{n(n+1)R^3}\right]^{1/2}\left[\int_{x_f}^1\left(\frac{-gA}{x^2}\right)^{1/2}dx\right]^{-1}. \tag{2.42}$$

We obtained the same result in Paper I, and were able there to analytically determine the parameter k_0, which was $\nu/2 - 1/6$ (ν being the polytropic index near the surface). Here however, k_0 must be evaluated by numerical integration, as we noted when introducing τ_0. Yet, as one may expect, this parameter varies only weakly with the frequency, so that the resonance periods are again evenly spaced, to first approximation.

What we have achieved so far is to relate the amplitude of the dynamical tide in the adiabatic interior to the total potential represented by the function Ψ. We now turn to the determination of this function Ψ, and more specifically to the evaluation of the normalized integral offset by the brackets in Eq. (2.40).

d) Approximate Solution for the Total Potential

To determine the total potential Ψ, we replace the perturbed density in the right-hand side of the Poisson equation (2.9) by its alternate from derived from the continuity equation, namely

$$\tilde{\varrho} = \frac{1}{g}\frac{d\varrho}{dr}\Psi - \frac{1}{g}\frac{d}{dr}(\varrho\chi) + \sigma^2\varrho a. \tag{2.43}$$

This permits us to rewrite Eq. (2.9) as

$$(x\Psi)'' - \left[\frac{n(n+1)}{x^2} + \frac{4\pi GR\varrho'}{g}\right](x\Psi) = -\frac{4\pi GRx}{g}\left[\frac{d(\varrho\chi)}{dx} - \sigma^2 R\varrho a\right]. \tag{2.44}$$

We can readily show that the right-hand side of this equation is negligible compared to the leading terms on the left-hand side, in the limit of small $\sigma^2 R/g_s$. This is certainly true in the convective core, where (2.8) demonstrates that $d\chi/dr$ is of the order of $\sigma^2 Ra$, which in turn is of the order of $\sigma^2 R\Psi/g$. In the radiative region, the ordering is a little less obvious; let us split there the oscillation into the equilibrium tide represented by $a_E = -\Psi/g$ and $\chi_E = 0$, and into the dynamical tide represented by a_D and χ_D. It is easily verified that, due to the factor σ^2, the term supplied by the equilibrium tide becomes negligible in the right-hand side of (2.44). As for the dynamical tide, its contribution to the solution has already been estimated in Paper I (I; 39) as

$$\Psi_D \sim -\frac{\sigma^2 R}{n(n+1)}\frac{3\varrho}{\bar{\varrho}}xa_D, \tag{2.45}$$

where $\bar{\varrho}(x)$ is the mean density inside the sphere of radius xR. Hence this contribution is also negligible, as long as the amplitude of the dynamical tide is of the order of (or is smaller than) that of the equilibrium tide. This will generally be the case in the presence of radiative dissipation, as we shall see in Section 4, the only exception being when a very close resonance is achieved with one of the first overtones.

We therefore reach the important conclusion that the density perturbation in the Poisson equation may be approximated by just retaining the first term in (2.43); in other words, to the lowest order in $\sigma^2 R/g_s$, the total potential is that calculated with the assumption of hydrostatic equilibrium. The expression $x^2\Psi/g$ is proportional to the function $Y(x)$ defined in Paper I (I; 33), and we showed that it is the regular solution of the differential equation (I; 38)

$$Y'' - 6\left(1 - \frac{\varrho}{\bar{\varrho}}\right)\frac{Y'}{x} - \left[n(n+1) - 12\left(1 - \frac{\varrho}{\bar{\varrho}}\right)\right]\frac{Y}{x^2} = 0. \tag{2.46}$$

The reader familiar with the subject of close binary stars recognizes this as an alternate form of Clairaut's equation, which permits one to calculate the constant of apsidal motion; this constant will be given later in terms of the surface values of Y and Y' (4.14).

© European Southern Observatory • Provided by the NASA Astrophysics Data System

1975A&A....41..329Z

We have thus established that the bracketed term in (2.40) is in fact just the coefficient H_n introduced in Paper I as

$$H_n = \frac{2n+1}{[(n-3)Y(1)+Y'(1)]X(x_f)} \int_0^{x_f} \left[Y'' - n(n+1)\frac{Y}{x^2} \right] X dx . \tag{2.47}$$

[We gave there an approximate value of that coefficient (I; 36), in which the apsidal motion constant was neglected compared to unity.] To calculate H_n, one has to integrate numerically both Eq. (2.46) through the whole star and the homogeneous form of (2.13) in the convective core.

e) Energy Flux

We have seen earlier (2.36) that the vertical displacement associated with the dynamical tide is given by

$$a_D = -K_s \varrho^{-1/2} x^{-2} (-gAx^{-2})^{-1/4} \cdot [(1-\gamma)\sin(\tau_s - \tau_0) + \gamma \exp i(\tau_s - \tau_0)] , \tag{2.48}$$

in the region far enough from both the surface and the convective core. The first term in the brackets represents a stationary wave, and this is the only one present in the adiabatic case ($\gamma = 0$). The second describes a travelling wave, whose phase velocity is directed towards the interior (with our choice of the exciting potential rotating in the direct sense).

This travelling wave carries a mechanical energy flux, since its pressure fluctuation is in quadrature with the radial displacement. Integrated over the sphere of radius r, this energy flux is given by

$$L_{\text{mech}} = \frac{2\pi}{2n+1} \frac{(n+m)!}{(n-m)!} \sigma r^2 \varrho \, \text{Im}(\chi a^*) . \tag{2.49}$$

This expression is similar to that derived by Baker and Kippenhahn (1962) for radial oscillations; a positive value means that the energy is flowing towards the surface.

An important property of this flux is its constancy in the region where a_D is represented by the asymptotic form (2.48). In that region, the flux can be expressed in terms of the amplitude constant K_0 (2.42), the damping factor γ, and the parameter ψ (2.37) as

$$L_{\text{mech}} = \frac{2\pi}{2n+1} \frac{(n+m)!}{(n-m)!} \frac{\sigma^2 R^3 (K_0)^2}{[n(n+1)]^{1/2}} \frac{\gamma}{\cos^2\psi + \gamma^2 \sin^2\psi} . \tag{2.50}$$

The constancy of the flux implies that the energy originates from below that region; this can be verified by replacing a and χ in (2.49) by their expressions valid in the convective core (2.17) and its vicinity (2.24). Such an energy input is required to maintain the oscillation at steady amplitude, since the energy transported by the travelling wave is dissipated in heat near the surface, where the departures from adiabacy become important. We have of course assumed that the amplitude of the tide remains constant in treating the frequency σ as a real quantity.

The source and the sink of the energy driving the dynamical tide are thus located in two distinct regions. It is clearly this property which permits us to adopt quite different solution approaches in the two regions, namely of solving (here in Section 2) the inhomogeneous adiabatic equations in the interior, and (in the next section) the homogeneous non-adiabatic system near the surface.

f) Surface Amplitude of the Oscillation

We will next evaluate the amplitude of the forced oscillation at the surface of the star. From the boundary condition (2.11) we can again deduce that the surface amplitude is composed of two parts, namely that due to the equilibrium tide

$$a_E = -\Psi(1)/g_s , \tag{2.51}$$

and that of the dynamical tide

$$a_D = \chi(1)/g_s . \tag{2.52}$$

If the oscillation were adiabatic in the whole star, the function $\chi(x)$ would be given by (I; 13) as

$$\chi = K \varrho^{-1/2} (-gAx^{-2})^{1/4} (\tau_s/2)^{1/2} J_\nu(\tau_s) . \tag{2.53}$$

The constant K can be easily related to the amplitude factor K_s in (2.34) by equating the asymptotic expression of (2.53) valid for large τ_s with that, derived from Eq. (2.34), of

$$\chi \sim \frac{\sigma^2 R}{n(n+1)} \frac{d}{dx}(x^2 a_D) . \tag{2.54}$$

The next step is to express this coefficient K_s in terms of K_0 and ψ; in the adiabatic case, (2.38) reduces to

$$K_s = -K_0/\cos\psi . \tag{2.55}$$

Finally, we find that the ratio $a_D(1)/a_E(1)$, which measures the surface amplitude of the dynamical tide compared to that of the equilibrium tide, is given by

$$a_D(1)/a_E(1) = D_n s^{4/3-\nu}/\cos\psi . \tag{2.56}$$

Here the coefficient D_n, which depends only on the order n of the considered spherical harmonic, is

$$D_n = \frac{3^{-1/6}\pi [n(n+1)]^{\nu/2 - 2/3}}{\Gamma(2/3)\Gamma(\nu+1)} \cdot \left(\frac{\varrho_f}{\varrho_s} \right)^{1/2} \left[\frac{R}{g_s} \left(\frac{-gA}{x^2} \right)' \right]_f^{-1/6} (RA_s)^{(\nu+1)/2} H_n , \tag{2.57}$$

with A_s and ϱ_s describing the behavior of A and ϱ near the surface (I; 16) as

$$A_s = \lim_{x \to 1} [-A(1-x)] , \quad \varrho_s = \lim_{x \to 1} [\varrho (1-x)^{-\nu}] . \tag{2.58}$$

© European Southern Observatory • Provided by the NASA Astrophysics Data System

1975A&A....41..329Z

This coefficient D_n is related to the resonance coefficient C_R used in Paper I

$$D_n=(\pi/2\Delta P)C_R\,, \tag{2.59}$$

and one verifies that the value of the amplitude between two consecutive resonances ($\cos\psi=\pm1$) is that which was given there. [A slight error occurred in the transcription of formula (35b) in Paper I, but the correct expression has been used for the numerical applications.]

Of course, this result applies only to the adiabatic case, but it is readily extended to the non-adiabatic situation by using for K_s the expression (2.38) which is valid there. We then obtain

$$a_D(1)/a_E(1)=D_n\delta s^{4/3-\nu}/(\cos\psi-i\gamma\sin\psi)\,. \tag{2.60}$$

Here γ is the damping constant introduced in expression (2.36); the complex factor δ is the ratio between the surface amplitudes of the actual dynamical tide and the hypothetical one calculated in the adiabatic approximation, both chosen to have the same interior amplitude as measured by K_0. These two parameters γ and δ, which are functions of the frequency s alone for a given model and a given integer n, have to be determined by the integration of the non-adiabatic equations through the outer part of the stellar envelope. This we will undertake in the next section.

Yet before we do so, let us briefly summarize what we have achieved so far in this section 2. We found that the oscillation excited by an outer harmonic potential is composed of two parts: the equilibrium tide, which can be predicted by assuming that the star is in hydrostatic equilibrium, and the dynamical tide, which reflects the pulsational properties of the star. This useful distinction between the two components of the forced oscillation was not possible in Paper I, where we chose to expand the solution in the free eigenmodes. The technique used here also permits a much easier generalization to the non-adiabatic case. An interesting result is that the radiative damping near the surface of the star affects the oscillation in the adiabatic interior in a way which can be described using essentially a single parameter γ, which we called the damping factor.

We now turn to the determination of this important damping factor, which requires the numerical integration of the functions representing the dynamical tide near the surface of the star.

3. The Oscillation in the Non-adiabatic Envelope

In this section, we will construct envelope solutions of the oscillation in the region below the surface where adiabacy can no longer be assumed. We recall that we have only to deal with the dynamical component of the oscillation, which in this region is just the solution of the equations governing the free oscillations; thus the excitation potential can be omitted as the source term from the full equations. The conservation of momentum, of mass and of energy are then expressed by

$$\frac{\partial^2\boldsymbol{r}}{\partial t^2}=-\frac{\nabla P}{\varrho}-\nabla\Phi\,, \tag{3.1}$$

$$\frac{\partial\varrho}{\partial t}+\varrho\nabla\cdot\boldsymbol{r}=0\,, \tag{3.2}$$

$$\nabla\cdot\boldsymbol{H}=Q_P\frac{\partial P}{\partial t}-\varrho C_P\frac{\partial T}{\partial t}\,. \tag{3.3}$$

In the usual notations, $\boldsymbol{r}$, P, ϱ, T and Φ are the position vector, the pressure, the density, the temperature, and the gravitational potential. The envelope is assumed to be in radiative equilibrium, so that the heat flux is given by

$$\boldsymbol{H}=-(4acT^3/3\kappa\varrho)\nabla T\,. \tag{3.4}$$

Here a and c are the radiation constants, C_P is the specific heat at constant pressure, κ the opacity, and Q_P is the logarithmic derivative of density with respect to pressure at constant temperature.

a) The Linearized Equations

We find it convenient to work in this section with a formalism similar to that used by Baker (1966), since it leads to a differential system which is somewhat more tractable for subsequent numerical integration. We again expand the fluctuations from the spherical equilibrium state in terms of the functions $Y_n^m(\theta,\phi,t)$ (2.4), so that the displacement vector and the fluctuation of the radiative flux are given by

$$\boldsymbol{\delta r}=r\mathrm{Re}\left[e(r)Y_n^m(\theta,\phi,t),\, b(r)\frac{dY_n^m}{d\theta},\, -imb\frac{Y_n^m}{\sin\theta}\right] \tag{3.5}$$

$$\boldsymbol{\delta H}=(L/4\pi r^2)\mathrm{Re}\left[(l(r)-2e(r))\right.$$
$$\left.\cdot\, Y_n^m(\theta,\phi,t),\, h(r)\frac{dY_n^m}{d\theta},\, -imh\frac{Y_n^m}{\sin\theta}\right]. \tag{3.6}$$

We then introduce the relative Lagrangian perturbation of pressure and temperature as

$$\delta_L P/P=\mathrm{Re}[p(r)Y_n^m(\theta,\phi,t)]\,,\qquad \delta_L T/T=\mathrm{Re}[t(r)Y_n^m]\,, \tag{3.7}$$

and define the two functions u and v which will represent their Eulerian perturbations as

$$\delta P/P=V(r)\mathrm{Re}[u(r)Y_n^m]\,,\qquad \delta T/T=V\nabla_{\mathrm{rad}}\mathrm{Re}[v(r)Y_n^m]\,. \tag{3.8}$$

The gradients V, ∇_{rad} and ∇_{ad} have the usual meaning

$$V=-\frac{\partial\ln P}{\partial\ln r},\qquad \nabla_{\mathrm{rad}}=\frac{\partial\ln T}{\partial\ln P},\qquad \nabla_{\mathrm{ad}}=\left(\frac{\partial\ln T}{\partial\ln P}\right)_S. \tag{3.9}$$

© European Southern Observatory • Provided by the NASA Astrophysics Data System

1975A&A....41..329Z

Since we are only interested in the outer region of the star, we omit the nuclear energy generation term; L is the constant luminosity flowing through the Lagrangian surface defined by Eq. (3.5) above, with a mean radius r. We shall also neglect the variation of the gravitational potential due to the non-sphericity of the mass distribution; the gravity then reduces to the radial vector

$$-\nabla\Phi=\left(-\frac{Gm}{(\boldsymbol{r}\cdot\boldsymbol{r})},0,0\right), \tag{3.10}$$

where m is the mass contained inside the same surface defined by (3.5).

We now linearize the Eqs. (3.1)–(3.3) and obtain, after elimination of b and h, the fourth-order differential system

$$\frac{du}{d\ln r}=\left(1+\sigma^2\tau_m^2-\frac{d\ln m}{d\ln r}\right)e-\left(Q_P-1-\frac{dV^{-1}}{d\ln r}\right)p+Q_T t\,, \tag{3.11}$$

$$\frac{dv}{d\ln r}=-l+e-(\kappa_P+Q_P)p+\left[4-\kappa_T+Q_T+\frac{d(V\nabla_{\rm rad})^{-1}}{d\ln r}\right]t, \tag{3.12}$$

$$\frac{de}{d\ln r}=-3e-Q_P p+Q_T t+\frac{n(n+1)}{\sigma^2\tau_m^2}u\,, \tag{3.13}$$

$$\frac{dl}{d\ln r}=-i\sigma\tau_t V(t-p\nabla_{\rm ad})-n(n+1)v\,. \tag{3.14}$$

We have written the coefficients of this system with the notation of Okamoto and Unno (1967), namely

$$Q_P=\left(\frac{\partial\ln\varrho}{\partial\ln P}\right)_T,\qquad Q_T=-\left(\frac{\partial\ln\varrho}{\partial\ln T}\right)_P, \tag{3.15a, b}$$

$$\kappa_P=\left(\frac{\partial\ln\kappa}{\partial\ln P}\right)_T,\qquad \kappa_T=\left(\frac{\partial\ln\kappa}{\partial\ln T}\right)_P, \tag{3.16a, b}$$

$$\tau_t=4\pi r^3 C_P\varrho T/LV\,,\qquad \tau_m=(r^3/Gm)^{1/2}\,. \tag{3.17a, b}$$

Prior to integrating the system, we must first express p and t in terms of u, v and e as

$$p=(u-e)V\,, \tag{3.18}$$

and

$$t=(v-e)V\nabla_{\rm rad}\,. \tag{3.19}$$

The functions e and u are related to those used in the preceding section: e is just the relative amplitude of the oscillation

$$e=a/r\,, \tag{3.20}$$

and u measures the Eulerian fluctuation of the pressure in non-dimensional units as

$$u=\chi/gr\,. \tag{3.21}$$

b) The Simplified Envelope Model

The outer part of the envelope can be considered to be a boundary layer whose role is to adjust the interior solution to the surface boundary conditions. We thus will make the following approximations, in order to both significantly simplify the differential system and to minimize the number of parameters needed to define the model:

i) At the surface, we take the crude boundary conditions $P=T=0$.

ii) Both the radiation pressure and the possible variation of the ionization state are neglected, so that $Q_P=Q_T=1$.

iii) The opacity coefficient is assumed to follow a power law in P and T; κ_P and κ_T are thus constants.

iv) The mass of the considered outer region is negligible compared to that of the whole star, therefore $d\ln m/d\ln r\ll 1$.

With these assumptions, the envelope has a polytropic stratification

$$\frac{\partial\ln P}{\partial\ln T}=v+1=\nabla_{\rm rad}^{-1}\,, \tag{3.22}$$

the polytropic index v being related to the exponents of the opacity coefficient through

$$v+1=(4-\kappa_T)/(1+\kappa_P)\,. \tag{3.23}$$

Further, the coefficients which remain in our differential system (3.11)–(3.14) can be expressed as

$$V=(v+1)/z\,,\qquad \sigma^2\tau_m^2=s^2x^3\,, \tag{3.24a, b}$$

$$\sigma\tau_t V=sPex^3(z/x)^{v+1}\,, \tag{3.25}$$

using, as before in Section 2, the fractional radius $x=r/R$, and the related depth $z=1-x$. The frequency is again measured in the dimensionless units of $s=(\sigma^2R^3/GM)^{1/2}$; the parameter Pe is the relevant Péclet number

$$Pe=\tfrac{5}{2}(GM^2/LR)(GM/R^3)^{1/2}C'\,, \tag{3.26}$$

which is closely related to the Kelvin-Helmholtz time measured in units of free fall time. Here C' is

$$C'=[4\pi R^4P(z)/GM^2](x/z)^{v+1}\,, \tag{3.27}$$

a constant in a polytropic model.

With all the assumptions stated above, a given envelope model can be defined by just three parameters. A convenient choice of such three is the polytropic index v, the Péclet number Pe, and one of the opacity exponents, say κ_P. These parameters may also be used to characterize more accurate models published in the literature; in that case v, κ_P and Pe, which are no longer constant, may be defined by some appropriate average.

© European Southern Observatory • Provided by the NASA Astrophysics Data System

1975A&A....41..329Z

c) Final Form of the Equations and Surface Boundary Conditions

With such a simplified polytropic model, and further using the property that $s \ll 1$, the differential system describing the dynamical tide in the envelope becomes

$$x\frac{du}{dz} = (v+1)^{-1}xp - t - e\,, \tag{3.28}$$

$$x\frac{dv}{dz} = l - v + (1+\kappa_P)p - (4-\kappa_T)t\,, \tag{3.29}$$

$$x\frac{de}{dz} = 3e + p - t - n(n+1)s^{-2}x^{-3}u\,, \tag{3.30}$$

$$x\frac{dl}{dz} = isPex^3(z/x)^{v+1}(t - p\nabla_{ad}) + n(n+1)v\,, \tag{3.31}$$

where

$$p = (v+1)(u-e)/z \quad \text{and} \quad t = (v-e)/z\,. \tag{3.32a, b}$$

At the surface ($z=0$), the Lagrangian perturbations must remain finite and therefore

$$u = v = e = 1\,, \tag{3.33}$$

having adopted the most natural normalization. The surface values for p and t are readily found as

$$p(0) = n(n+1)s^{-2} - 4 \tag{3.34}$$

$$t(0) = (v+1)^{-1}[n(n+1)s^{-2} - 4 + (1+\kappa_P)^{-1}l(0)]\,. \tag{3.35}$$

The remaining surface value $l(0) = l_0$ will be determined as an eigenvalue through the numerical integration of the system. The last boundary condition will be applied at the other end of the integration domain, as a matching condition between the envelope (non-adiabatic) and the interior (adiabatic) solutions. But before we establish that condition, we need to know the asymptotic form of the envelope solution in the region where the matching will be performed.

d) Asymptotic Behavior of the Solution

The differential equations (3.28) and (3.30), together with the condition $t = p\nabla_{ad}$, describe the behavior of the adiabatic oscillation which has been considered in Paper I. For a long enough period (or small enough s), one can apply the asymptotic method used there which leads us to express the function u, near the surface, as

$$u = \Gamma(v+1)\,[n(n+1)Bs^{-2}]^{-v/2-1/4} \cdot x^{v/2-1/4}z^{-v/2-1/4}(\tau_s/2)^{1/2}J_v(\tau_s)\,. \tag{3.36}$$

This is equivalent to Eq. (2.53). With the assumptions made above, the argument τ_s becomes

$$\tau_s = [n(n+1)Bs^{-2}]^{1/2}\int_0^z x^{-5/2}z^{-1/2}dz \tag{3.37}$$

where for brevity

$$B = (v+1)\nabla_{ad} - 1\,. \tag{3.38}$$

The function u has been normalized in order to satisfy the surface boundary condition $u=1$; the quantity B is a positive constant in a radiative polytropic model, as considered here. Far enough from the surface, we can again replace the Bessel function by the leading term of its asymptotic expansion, and thus obtain

$$u = \pi^{-1/2}\Gamma(v+1)\,[n(n+1)Bs^{-2}]^{-v/2-1/4} \cdot x^{v/2-1/4}z^{-v/2-1/4}\cos(\tau_s - v\pi/2 - \pi/4)\,. \tag{3.39}$$

Such a solution is only relevant for an oscillation which is adiabatic throughout the star. In the non-adiabatic case, the function u takes the more general form

$$u = \pi^{-1/2}\Gamma(v+1)\,[n(n+1)Bs^{-2}]^{-v/2-1/4}x^{v/2-1/4} \cdot z^{-v/2-1/4}\delta^{-1}[\cos(\tau_s - \tau_0) - i\gamma\sin(\tau_s - \tau_0)]\,, \tag{3.40}$$

as we have seen in Section 2. Similarly, since according to (3.30) $de/dz \sim -n(n+1)s^{-2}x^{-4}u$, the relative amplitude becomes

$$Be = -\pi^{-1/2}\Gamma(v+1)\,[n(n+1)Bs^{-2}]^{-v/2+1/4}x^{v/2-7/4} \cdot z^{-v/2+1/4}\delta^{-1}[\sin(\tau_s - \tau_0) + i\gamma\cos(\tau_s - \tau_0)]\,, \tag{3.41}$$

which is equivalent to expression (2.48) of Section 2. The asymptotic expressions above will be used to evaluate the parameters γ, δ and τ_0 by comparison with the solution obtained by numerical integration.

e) Interior Boundary Condition

We have yet to establish a fourth boundary condition to be imposed upon the solution that represents the dynamical tide in the envelope. In the deep interior, the oscillation becomes adiabatic and the Lagrangian fluctuations of temperature and pressure are related by $t = p\nabla_{ad}$. But such a condition should not be asserted close to the surface, since there departures from adiabacy may not be negligible. We therefore impose instead the milder condition that

$$t = p\nabla_{ad} + \Delta t\,, \tag{3.42}$$

in which the correction Δt is small enough, compared to t, to be evaluated by some approximate method. Since Eq. (3.31) yields

$$\Delta t = \frac{1}{isPex^3}\left(\frac{x}{z}\right)^{v+1}\left[x\frac{dl}{dz} - n(n+1)v\right], \tag{3.43}$$

we can derive a first approximation for Δt by just replacing l in this expression by its leading term for small s, which is

$$l \sim n(n+1)Bs^{-2}x^3u\,, \tag{3.44}$$

obtained by replacing v by its approximate value $-Be$ in (3.12). Thus to the lowest order in s, the correction term Δt is given by

$$\Delta t = if(z)Be/z\,, \tag{3.45}$$

© European Southern Observatory • Provided by the NASA Astrophysics Data System

1975A&A....41..329Z

where

$$f(z)=\frac{n(n+1)B}{Pes^3x^6}\left(\frac{x}{z}\right)^{v+1}. \tag{3.46}$$

This function $f(z)$ turns out to be a convenient measure for the departure from adiabacy, since $|\Delta t/t|=fB/(B+1)$. Due to the large value of the Péclet number Pe, $f(z)$ is very small in the deep interior, but it increases without bound as one approaches the surface.

To improve the accuracy of the correction Δt, we will have to include terms of higher order in s, and also terms of order Pe^{-1}. This requires the ordering of all the functions entering the differential system; in doing so, we find readily that u has the lowest order in s^{-1}, that $|v|$, $|e|$, $|p|$ and $|t|$ are of order $s^{-1}|u|$, whereas $|l|$ is of order $s^{-2}|u|$. Omitting the details, let us simply write down the expression for Δt to the next order of approximation as

$$\Delta t=-if\{(1+if)^2Be/z+[(v+1)\kappa_P-B]u/z\}. \tag{3.47}$$

Likewise, the fluctuating luminosity then becomes

$$l=B[(1+if)n(n+1)s^{-2}x^{-3}u+\kappa_P p-4e]. \tag{3.48}$$

Introducing the improved expression (3.47) for Δt into (3.42), we obtain a homogeneous relation between the function p, t, (or u, v) and e. This relation will be used as the fourth boundary condition for the differential system, to be applied at the bottom of the integration domain.

f) Numerical Integration

We integrated the fourth-order differential system (3.28)–(3.31) by a shooting method, using essentially the same technique as Baker and Kippenhahn (1962), when solving for the radial oscillations in a Cepheid envelope. The model having been specified by the parameters v, κ_P and Pe, and the frequency s being fixed, the set of initial values at the surface ($u=v=e=1$) was completed by an arbitrarily chosen $l(0)=l_0$. The system was then integrated to some depth z_m, where we sought to satisfy the last boundary condition derived above, (3.42) with (3.47).

Since the equations are linear, in principle only three integrations would be necessary to determine the complex eigenvalue l_0 by linear interpolation. But to actually realize this, a very accurate integration method must be used, with the same sequence of spatial steps taken in each of the integrations. The algorithm we chose was that of Burlisch and Stoer (1966), as implemented by Hénon (1967).

The depth z_m at which the fourth boundary condition is applied was selected so as to minimize the difference between the value of $l(z)$ obtained by integration and that predicted in the quasi-adiabatic approximation by (3.48). At first sight, it is not clear why such an optimum depth should even exist; on the contrary, one might expect the two values of $l(z)$ to move closer as the integration proceeds further into the star. However, the fourth-order system admits also a diffuse solution; one branch of which is an exponentially growing function. The e-folding length of this diverging solution can be estimated by letting $u=e=0$ in the differential system; one finds that the ratio of this length to the wavelength of the forced oscillation is just $[f(z)/\pi]^{1/2}$. Since $f(z)$ is a rapidly decreasing function with depth, the growth rate of the diverging branch becomes eventually so high that its presence can no longer be avoided in the numerical integration of the solution. Baker and Kippenhahn encountered the same difficulty, and they too stopped their integrations at a rather moderate depth.

The optimal depth z_m of the integration domain varied, as expected, with the degree of non-adiabacy: it increased with period and decreased with the Péclet number. Using the higher accuracy expression (3.47) for Δt, we were able in most cases to keep the difference between the two values of $l(z_m)$ below one percent.

Once the eigenvalue l_0 was determined, the differential equations in u and e, (3.28) and (3.30), were integrated beyond the depth z_m using the quasi-adiabatic approximation. By this we mean that p and t were related by Eq. (3.42), and that Δt was evaluated by (3.47). The integration was continued until the functions u and e approached their asymptotic form, as predicted by Eqs. (3.40) and (3.41). The complex amplitude reduction factor δ was then evaluated by comparison with the adiabatic solution, whereas the damping constant γ was derived from the identity

$$\frac{2\gamma}{1+\gamma^2}=\frac{[n(n+1)z/Bs^2x^3]^{1/2}(ue^*-u^*e)}{[n(n+1)z/Bs^2x^3]uu^*+ee^*}, \tag{3.49}$$

obtained by combining (3.40) and (3.41).

We now turn to the following section, where we will present the results of those numerical integrations.

4. Results and Discussion

The zero age main-sequence models used for the numerical integrations have been calculated by Aizenman (1974) with a simplified stellar structure code. The bound-free opacity coefficient was approximated by an unmodified Kramer law, and therefore the models at low masses differ somewhat from those constructed with more realistic opacities. However we feel that these models are accurate enough for our purposes; before going into further refinements, one should for instance include the Coriolis force in the present analysis.

The envelopes of these models are well represented by the parameters $v=3.25$ and $\kappa_P=1$; their other relevant properties are listed in Table 1, together with the results of our integrations. We calculated the constant

© European Southern Observatory • Provided by the NASA Astrophysics Data System

1975A&A....41..329Z

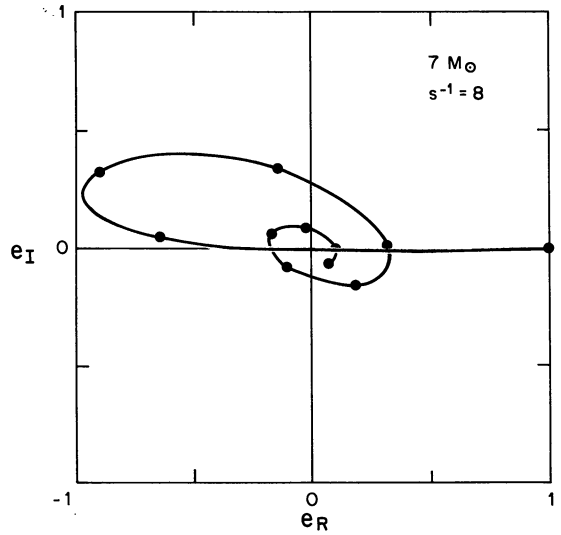

Fig. 1. The variation of the relative amplitude of the forced oscillation with depth z, in the envelope of a zero age main-sequence star of 7 $M_\odot$, for the dimensionless period $s^{-1}=8$. The complex eigenfunction $e(z)$ is normalized to 1 at the surface ($z=0$); the real part is in abscissae, the imaginary part in ordinates. Between two consecutive dots, the fractional depth is incremented by 0.02; the curve stops at $z=0.20$

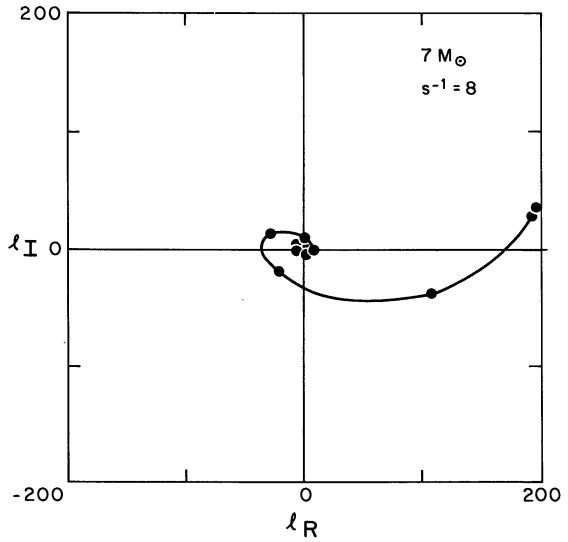

Fig. 2. The same as Fig. 1, but showing the variation of the complex eigenfunction for the relative flux perturbation, l, with depth z

H_n, which enters in D_n (2.57) and E_n (4.17), for the spherical numbers $n=2$, 3 and 4. The integration of the envelope solution was performed only for $n=2$, which characterizes the dominant term of the Fourier expansion of the tidal potential in a binary system.

Let us recall that the frequency s, or σ in its dimensional form, is that of the excitation potential. When this outer potential rotates with the angular velocity ω, which in a binary system is the orbital velocity, and when the star itself rotates with the velocity Ω with respect to an inertial frame, the excitation frequency is $\sigma=m(\omega-\Omega)$, the apparent period of the tide being $2\pi/|\sigma|$. Whenever the azimuthal number m needs to be specified, we will present the results with the particular choice $m=2$, which corresponds to the dominant term in the tidal potential.

Figures 1 and 2 show the complex eigenfunctions $e(z)$ and $l(z)$ in the envelope of a 7 $M_\odot$ star, for a typical case: the dimensionless period is $s^{-1}=8$, corresponding here to a damping factor γ of about one half. Notice the reasonable behavior of the eigenfunctions near the surface, which seems to indicate that the fairly crude surface conditions of the envelope model, namely $P=T=0$, are here acceptable. The vertical amplitude, represented by the modulus of $e(z)$, goes through a sharp minimum at $z=1.02\,10^{-2}$, which is slightly deeper than the first node of the adiabatic oscillation ($z=0.95\,10^{-2}$). In contrast, the fluctuating luminosity barely changes over that first interval.

a) Damping Constant and Amplitude Reduction Factor

The variation with period of the damping constant γ and the modulus of the amplitude reduction factor $|\delta|$ are shown in Fig. 3 for four different models, of 1.6, 3, 7 and

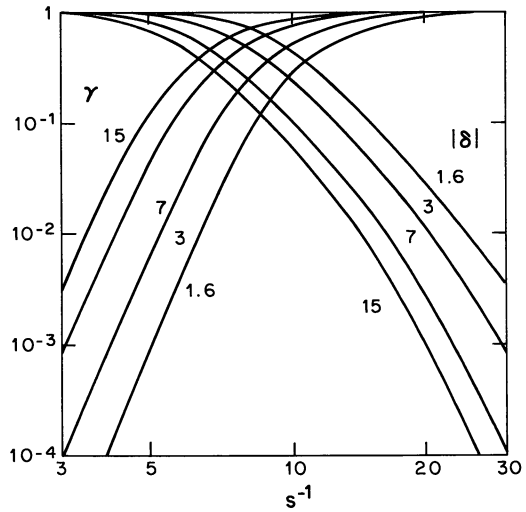

Fig. 3. The damping constant, γ, and the module of the amplitude reduction factor, $|\delta|$, versus the dimensionless period s^{-1}, for models of 1.6, 3, 7 and 15 $M_\odot$. One follows in this diagram how the behavior of the oscillation gradually changes, with period, from adiabatic (γ negligible, $\delta\sim 1$) to non-adiabatic ($\gamma\sim 1$, δ negligible)

15 $M_\odot$. Notice that to first approximation the curves are superposable along the s-axis. This is so because the properties of the fourth-order differential system depend chiefly on a single parameter, which is $[n(n+1)B]^{-(\nu+1)}Pes^{2\nu+5}$. Since the Péclet number of the envelope decreases with the mass of the star, the massive stars are those which exhibit the strongest non-adiabatic behavior, for a given dimensionless period.

Let us describe in some detail the results for a star of 7 $M_\odot$. The departures from adiabacy, as measured by $|\delta|$, are negligible as long as s^{-1} is smaller than about 5, which is the period of the fourteenth overtone in that star. Thereafter, the amplitude drops sharply

© European Southern Observatory • Provided by the NASA Astrophysics Data System

1975A&A....41..329Z

with increasing period; if falls below one hundredth of the value predicted by the adiabatic approximation at $s^{-1}=16$.

As expected, the damping constant varies in the opposite way: negligible for small periods, γ increases rapidly and approaches unity when s^{-1} reaches 10. For longer periods, the forced oscillation behaves like a purely traveling wave, as demonstrated by Eq. (2.48) with $\gamma=1$, and the resonances are smoothed out in a manner reminiscent of multiresonance in nuclear physics. This can be seen in the surface amplitude results to be presented next.

b) Surface Distortion

We have already evaluated, in (2.60), the ratio between the surface amplitudes of the dynamical tide and the equilibrium tide; let us take here the modulus of that ratio

$$\alpha(s)=\frac{|a_D(1)|}{a_E(1)}=\frac{D_n|\delta|s^{4/3-\nu}}{(\cos^2\psi+\gamma^2\sin^2\psi)^{1/2}}, \tag{4.1}$$

where ψ is the argument defined earlier in (2.37), which varies linearily with period to first approximation as

$$\psi(s)=(\pi/\Delta P)s^{-1}-(\pi/12)-\tau_0(s)\,. \tag{4.2}$$

Since γ and δ, as we have seen, vary moderately with period compared to ψ, this ratio α is maximum for $\psi=\pi/2+k\pi$, where $s=s_k$ [see (2.41)]. At the peak of a resonance, the value of α is therefore (for $n=2$)

$$\alpha_{\max}=\alpha(s_k)=D_2|\delta|s_k^{4/3-\nu}/\gamma\,. \tag{4.3}$$

At the midpoint between two consecutive resonances, where $\psi=k\pi$ and $s^{-1}=s_{k+1/2}^{-1}=\frac{1}{2}(s_k^{-1}+s_{k+1}^{-1})$, the amplitude ratio goes through a minimum

$$\alpha_{\min}=\alpha(s_{k+1/2})=D_2|\delta|s_{k+1/2}^{4/3-\nu}\,. \tag{4.4}$$

We found the same result for $\alpha_{\min}$ in Paper I, where of course the amplitude reduction factor was unity. In that adiabatic case, the function $s^{4/3-\nu}$, due to its negative exponent, was responsible for the diverging surface amplitudes as $s^{-1}\to 0$; here however the behavior of $\alpha_{\min}$ is dominated by the rapid decrease of δ with period.

In Fig. 4, $\alpha_{\max}$ and $\alpha_{\min}$ are plotted versus the dimensionless period s^{-1}, for a $7\,M_\odot$ star; those curves are the envelopes of the actual function $\alpha(s)$ which is difficult to represent as such because the resonances are very closely spaced. The distance between the two curves decreases with increasing period; it becomes so small after $s^{-1}\sim 15$ that there is no visible sign left of the resonances.

The median curve denoted by $\bar{\alpha}$, which lies between the loci of $\alpha_{\max}$ and $\alpha_{\min}$, is defined by $|\cos\psi|=1/\sqrt{2}$. It has the following meaning: Assuming a random distribution of the periods, in some hypothetical sample, the ratio α would lie above that median curve in half of the cases, and below it in the other half. Given such a distribution, the median curve is therefore the locus of the most probable value of the amplitude ratio.

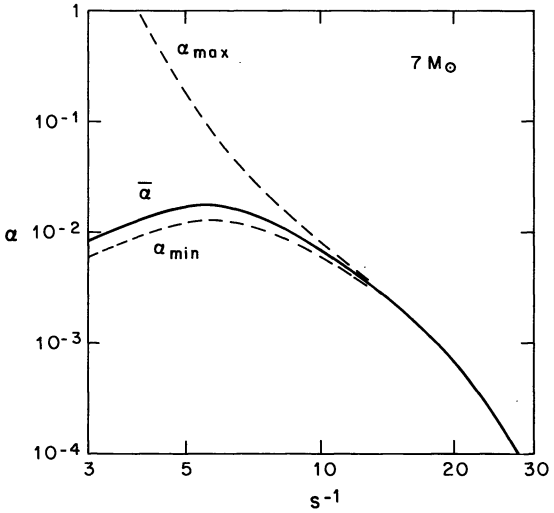

Fig. 4. The ratio α of the surface amplitudes of the dynamical to the equilibrium tide, plotted as a function of the non-dimensional period s^{-1} for a $7\,M_\odot$ star. The upper and lower (dashed) curves are the loci of the maxima and the minima of that ratio α, which are attained respectively at the peak of a resonance and at the midpoint between two resonances. The median curve is the locus of the most probable value, $\bar{\alpha}$. as defined in the text. Notice that α is in general small compared to unity, but that for $s^{-1}<4$ the amplitude of the dynamical tide at resonance is larger than that of the equilibrium tide

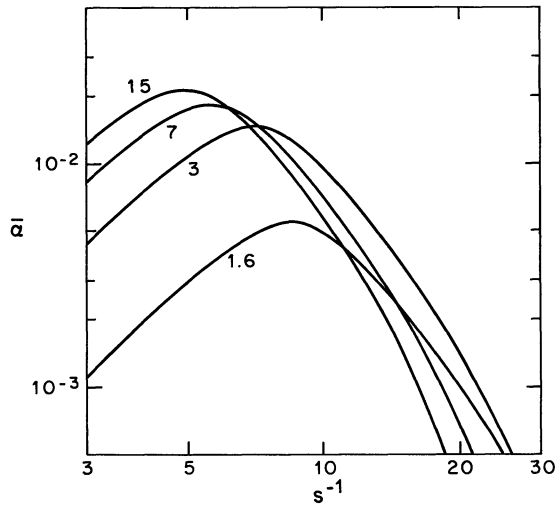

Fig. 5. The median value of the amplitude ratio, $\bar{\alpha}$, versus period s^{-1}, for the same four models as in Fig. 3, with masses 1.6, 3, 7 and 15 $M_\odot$. Notice that the deformation due to the dynamical tide increases with the mass of the star

In Fig. 5, we show only this median curve $\bar{\alpha}$, but this time for the four different models already used in Fig. 3. The relatively small values of $\bar{\alpha}$ reached at the maximum of the curves indicate that the bulge created by the dynamical tide is in general negligible compared to that due to the equilibrium tide. Such an additional distortion would probably only be observable at the peak of a resonance, and provided that the excitation period is

© European Southern Observatory • Provided by the NASA Astrophysics Data System

1975A&A....41..329Z

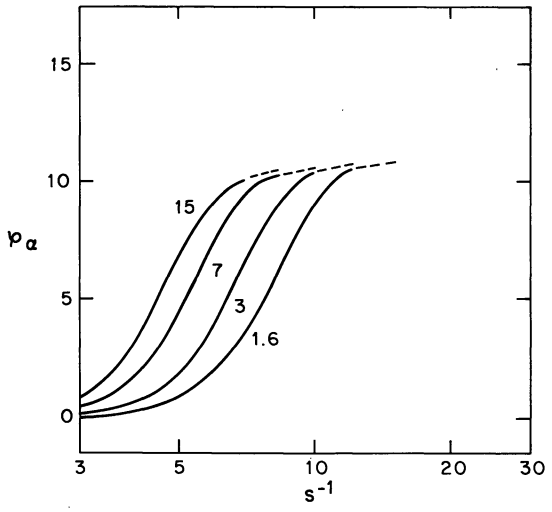

Fig. 6. The phase lag ϕ_α (in degrees) of the tidal bulge created by the dynamical tide, at the midpoint between two resonances, versus period s^{-1}. The dashed line indicates that the computational accuracy deteriorates there because the oscillation becomes an almost purely travelling wave

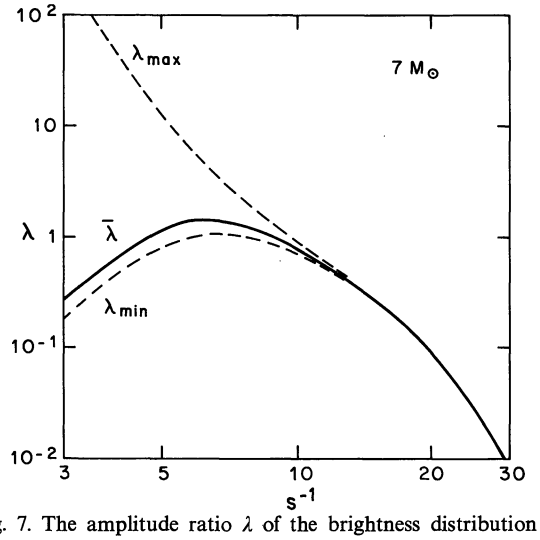

Fig. 7. The amplitude ratio λ of the brightness distribution of the dynamical tide to that of the equilibrium tide, plotted versus period s^{-1} for a 7 $M_\odot$ star. The dashed curves are the loci of the maxima and minima of λ; the median curve is the locus of the most probable value $\bar{\lambda}$. Notice that over a broad range of periods the ratio λ is of order unity, indicating departures from Von Zeipel's gravity-darkening law which should be observable

small enough; the latter would however imply a severe lack of synchronism. We should remark that for massive stars this extra deformation can be of the same order as that which is induced by the non-sphericity of the inner mass distribution of those stars and which is measured by the constant of apsidal motion; this is true over a broad range of apparent periods.

The phase lag of the bulge due to the dynamical tide, with respect to the exciting potential, is given by

$$\phi = \tfrac{1}{2}\{\text{atan}[\text{Im}(\delta)/\text{Re}(\delta)] - \text{atan}(\gamma \tan\psi)\} \qquad (4.5)$$

(again for the spherical numbers $n=m=2$). This is also a function of period, primarily through ψ since γ and δ are fairly insensitive to period. At midpoint between two resonances of periods s_k^{-1} and s_{k+1}^{-1}, the phase lag assumes the value $\phi_\alpha + k\pi/2$, with

$$\phi_\alpha = \tfrac{1}{2}\,\text{atan}[\text{Im}(\delta)/\text{Re}(\delta)]\,. \qquad (4.6)$$

This function ϕ_α is represented in Fig. 6 for the same four stellar models as in Fig. 3 and 5.

c) Surface Brightness Distribution

Similarly, one can compare the flux distribution due to the dynamical tide, $\text{Re}\{F_D P_2^2(\cos\theta)\exp 2i\phi\}$, with that caused by the equilibrium tide, $F_E P_2^2(\cos\theta)\cos 2\phi$. The relative value of F_D is just the modulus of the eigenvalue l_0 determined by numerical integration, if the surface amplitude of the dynamical tide is normalized to unity. Scaling this flux with the actual value of the surface amplitude, one gets

$$F_D = (L/4\pi R^2) l_0(a_D(1)/R)\,. \qquad (4.7)$$

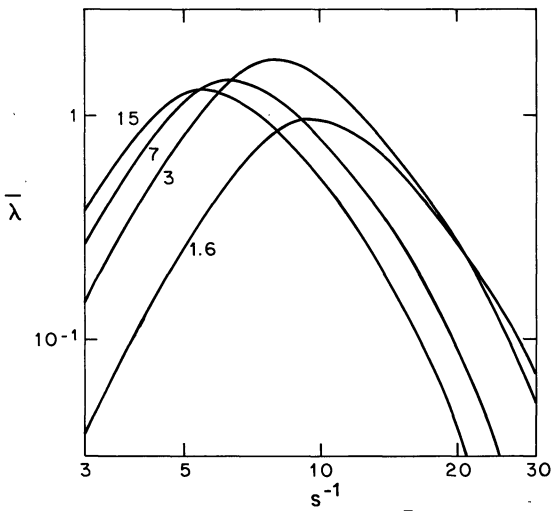

Fig. 8. The median value of the flux ratio, $\bar{\lambda}$, versus period s^{-1}, for the same four models as in Fig. 3, with masses 1.6, 3, 7 and 15 $M_\odot$. The maximum value of $\bar{\lambda}$ is weakly model dependent; stars of about 3 $M_\odot$ will on the average exhibit slightly larger departures from Von Zeipel's law

The equilibrium flux is related to the equilibrium surface distortion by Von Zeipel's theorem, which states that the flux is proportional to the local gravity; hence

$$F_E = -(L/4\pi R^2) 2(a_E(1)/R)\,. \qquad (4.8)$$

The modulus of the complex ratio between F_D and F_E is thus given by

$$\lambda(s) = |F_D/F_E| = |l_0(s)|\alpha(s)/2\,. \qquad (4.9)$$

Figure 7 represents the variations of the extreme values of that ratio $\lambda(s)$ for the 7 $M_\odot$ star, together with its median value $\bar{\lambda}$ which is the most probable value defined as above for α. In Fig. 8, the median curve

© European Southern Observatory • Provided by the NASA Astrophysics Data System

1975A&A....41..329Z

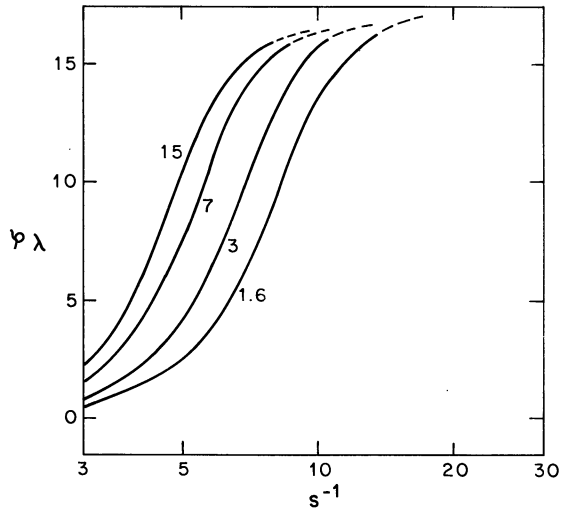

Fig. 9. The phase lag ϕ_λ of the flux distribution created by the dynamical tide, at the midpoint between two resonances, versus period s^{-1}, for the same models with masses 1.6, 3, 7 and 15 $M_\odot$

alone is shown as it varies with period for the four different models.

One sees that the modification of the brightness distribution due to the dynamical tide can be quite important. For the 7 $M_\odot$ star, the deviation from Von Zeipel's gravity-darkening law exceeds 10% as soon as the apparent period becomes smaller than 20 in dimensionless units, or 4.36 days in physical units. To illustrate this further, such a period would be experienced by a star of 7 $M_\odot$ with an orbital period of 3 days and a departure from synchronism of 35%, or else with an orbital period of 2 days and 23% of such a departure.

Moreover, the brightness distribution in general loses its East-West symmetry (for an observer orbiting with the companion star). This occurs because it can take any possible orientation relative to the tidal potential, depending on the excitation period, as can be seen from (4.7) which yields a phase lag of

$$\phi = \tfrac{1}{2}\{\mathrm{atan}[\mathrm{Im}(\delta)/\mathrm{Re}(\delta)]\} + \mathrm{atan}[\mathrm{Im}(l_0)/\mathrm{Re}(l_0)] - \mathrm{atan}(\gamma\tan\psi)\}\,. \tag{4.10}$$

At midpoint between two resonances, this phase lag is $\phi_\lambda + k\pi/2$, where

$$\phi_\lambda = \phi_\alpha + \tfrac{1}{2}\,\mathrm{atan}[\mathrm{Im}(l_0)/\mathrm{Re}(l_0)]\,. \tag{4.11}$$

Figure 9 shows the variations of this angle ϕ_λ as a function of the period s^{-1} for the four different models.

Statistically, the largest modification of the flux distribution should be expected near the maximum of the median curve in Fig. 8. For a 7 $M_\odot$ star, this maximum occurs at $s^{-1}=6.2$, which already corresponds to a fairly large deviation from synchronism. For example, it would be the tidal period on a star of that mass in a 2.7 days period orbit, if it rotates with twice the velocity required for synchronism.

There are several observable consequences of this lag of the brightness distribution. We shall discuss these in a subsequent paper.

e) Gravitational Field Created by the Perturbed Mass Configuration

Outside the star, the gravitational field resulting from the tidally distorted mass distribution is described by the potential

$$V = \mathrm{Re}[\Phi(1)Y_n^m(\theta,\phi,t)]x^{-(n+1)}\,. \tag{4.12}$$

Using Poisson's equation in the form of (2.44), and remembering that $\Psi = \Phi + U_n^m x^n$ as in Eq. (2.5), one can express the surface value of Φ by an integral over the star. Proceeding as in Paper I we obtain

$$\Phi(1) = \Phi_E(1) + \Phi_D(1) = \frac{(n+4)Y(1) - Y'(1)}{(n-3)Y(1) + Y'(1)} U_n^m + \frac{1}{(n-3)Y(1)+Y'(1)} \frac{4\pi R^3}{M} \cdot \int_0^{x_f} Y(x)\left[\frac{d}{dx}(\varrho\chi) - \sigma^2 R\varrho a\right] dx\,. \tag{4.13}$$

The first term, $\Phi_E(1)$, measures the exterior potential created by the equilibrium tide; thus for $n=2$, the factor multiplying U_n^m is just twice the apsidal motion constant k, namely

$$2k = \frac{6Y(1) - Y'(1)}{Y'(1) - Y(1)}\,. \tag{4.14}$$

Numerical values of that constant are given in Table 1 for the stellar models used here.

The second term, $\Phi_D(1)$, proceeds from the dynamical tide, and involves an integral which has already been evaluated in Paper I (I; 30); the result was expressed there in (I; 34) in terms of a constant K which measured the amplitude of the oscillation. This constant K is readily related to the factor $(K_c + N_1)$ which plays here the same role. Comparing the asymptotic expressions (I; 24a) and (2.30), we find that

$$K = -\left[\frac{\pi}{2}\frac{\sigma^2}{n(n+1)}\right]^{1/2} R(K_c + N_1)\,. \tag{4.15}$$

We have evaluated earlier $(K_c + N_1)$ in terms of ψ and K_0 in (2.39); substituting for K_0 its value (2.40), we can express the dynamical tide contribution $\Phi_D(1)$ as

$$\Phi_D(1) = U_n^m E_n s^{8/3}[q(s) + ip(s)]\,, \tag{4.16}$$

with

$$E_n = \frac{3^{8/3}[\Gamma(4/3)]^2}{(2n+1)\,[n(n+1)]^{4/3}} \left(\frac{\varrho_f R^3}{M}\right)\left[\frac{R}{g_s}\left(\frac{-gA}{x^2}\right)'_f\right]^{-1/3} (H_n)^2\,. \tag{4.17}$$

The complex function $q(s) + ip(s)$ of (4.17) is given by

$$q(s) + ip(s) = \frac{2}{\sqrt{3}} \frac{\cos(\psi - \pi/3) - i\gamma\sin(\psi - \pi/3)}{\cos\psi - i\gamma\sin\psi}\,; \tag{4.18}$$

© European Southern Observatory • Provided by the NASA Astrophysics Data System

1975A&A....41..329Z

Table 1. Numerical results for zero age main-sequence stars

Mass (in solar units)		M	1.6	2	3	5	7	10	15
Radius (in solar units)		R	1.152	1.294	1.678	2.350	2.919	3.652	4.672
Fractional radius of convective core		x_f	0.1251	0.1594	0.1854	0.2143	0.2379	0.2669	0.3054
Péclet number of envelope (3.26)		Pe	$1.24\ 10^{12}$	$5.75\ 10^{11}$	$1.39\ 10^{11}$	$2.68\ 10^{10}$	$1.19\ 10^{10}$	$5.26\ 10^{9}$	$2.73\ 10^{9}$
Momentum of inertia (in MR^2 units)		I/MR^2	$7.57\ 10^{-2}$	$7.71\ 10^{-2}$	$7.95\ 10^{-2}$	$8.35\ 10^{-2}$	$8.72\ 10^{-2}$	$9.13\ 10^{-2}$	$9.59\ 10^{-2}$
Apsidal motion constant (4.15)		k	$1.37\ 10^{-2}$	$1.43\ 10^{-2}$	$1.52\ 10^{-2}$	$1.69\ 10^{-2}$	$1.86\ 10^{-2}$	$2.07\ 10^{-2}$	$2.31\ 10^{-2}$
Dimensionless period corresponding to 1 day		s^{-1}	8.838	8.305	6.891	5.365	4.586	3.917	3.316
Interval between eigenperiods (2.42)	$n=2$	ΔP	0.2408	0.2623	0.2865	0.3249	0.3635	0.4207	0.5159
	$n=3$		0.1703	0.1855	0.2026	0.2298	0.2571	0.2975	0.3648
	$n=4$		0.1319	0.1437	0.1569	0.1780	0.1991	0.2304	0.2825
Tidal amplitude constant (2.57)	$n=2$	D_n	$9.93\ 10^{-5}$	$2.36\ 10^{-4}$	$3.85\ 10^{-4}$	$5.73\ 10^{-4}$	$7.29\ 10^{-4}$	$9.02\ 10^{-4}$	$1.10\ 10^{-3}$
	$n=3$		$2.39\ 10^{-5}$	$7.25\ 10^{-5}$	$1.39\ 10^{-4}$	$2.39\ 10^{-4}$	$3.38\ 10^{-4}$	$4.67\ 10^{-4}$	$6.46\ 10^{-4}$
	$n=4$		$4.84\ 10^{-6}$	$1.88\ 10^{-5}$	$4.19\ 10^{-5}$	$8.34\ 10^{-5}$	$1.31\ 10^{-4}$	$2.03\ 10^{-4}$	$3.19\ 10^{-4}$
Tidal torque constant (4.18)	$n=2$	E_n	$2.41\ 10^{-9}$	$1.45\ 10^{-8}$	$4.72\ 10^{-8}$	$1.53\ 10^{-7}$	$3.80\ 10^{-7}$	$1.02\ 10^{-6}$	$3.49\ 10^{-6}$
	$n=3$		$1.03\ 10^{-11}$	$1.02\ 10^{-10}$	$4.51\ 10^{-10}$	$1.97\ 10^{-9}$	$6.05\ 10^{-9}$	$2.04\ 10^{-8}$	$9.14\ 10^{-8}$
	$n=4$		$6.17\ 10^{-14}$	$9.96\ 10^{-13}$	$6.00\ 10^{-12}$	$3.53\ 10^{-11}$	$1.34\ 10^{-10}$	$5.69\ 10^{-10}$	$3.32\ 10^{-9}$

its real and imaginary parts are respectively

$$q(s)=\frac{1}{\sqrt{3}}+\frac{(1-\gamma^2)\sin\psi\cos\psi}{\cos^2\psi+\gamma^2\sin^2\psi} \tag{4.19}$$

and

$$p(s)=\frac{\gamma}{\cos^2\psi+\gamma^2\sin^2\psi}. \tag{4.20}$$

For $n=2$, the expression $\frac{1}{2}E_n s^{8/3}q(s)$ can be considered as the apsidal motion constant due to the dynamical tide. Because of the small value of E_2 (see Table 1), this contribution is in general negligible. It is only at the peak of a weakly damped resonance that the dynamical tide could possibly be noticed in the apsidal motion of a close binary system; the probability of observing such an event is however very small.

In contrast, the imaginary part p can be much more easily detected in such a system, since it produces a torque which, applied to the star, tends to synchronize its rotation with the orbital motion, as we shall next see. If the orbit is not circular, this p will also be responsible for the secular evolution of the orbital eccentricity.

f) Applied Torque

When some dissipative process is at work, a torque is applied to the star, due to the fact that the mass configuration has no longer the same symmetry properties as the total potential. To evaluate it, one could take the torque applied to the elementary volume dv,

$$d\Gamma=\mathrm{Re}[\tilde{\varrho}\,Y_n^m(\theta,\phi,t)]\cdot\mathrm{Re}\left[\Psi\frac{d}{d\phi}Y_n^m(\theta,\phi,t)\right], \tag{4.21}$$

and integrate that over the whole star. In writing (4.21) we assumed that the exciting potential reduces to a single Fourier component; otherwise $d\Gamma$ would involve a double summation over all components.

An alternate method for calculating the total torque makes use of the expression of the external potential in (4.12). In a circular orbit, the exciting potential produced by the companion of mass qM is just

$$U_2^2=-\tfrac{1}{4}\frac{GqM}{R}\left(\frac{R}{D}\right)^3, \tag{4.22}$$

D being the separation of the two stars. The tangential force applied to the companion is

$$f_\phi=-\frac{qM}{D}\frac{\partial V}{\partial\phi} \tag{4.23}$$

evaluated at $2\phi=\sigma t$, and its moment with respect to the star under consideration is equal and opposite to the torque Γ experienced by that star, so that

$$\Gamma=-Df_\phi=\tfrac{3}{2}Mg_sRq^2\left(\frac{R}{D}\right)^6E_2s^{8/3}p(s). \tag{4.24}$$

One can readily verify that the work done per unit time by this torque, against the outer potential rotating with the phase velocity $\sigma/2$, is identical to the integrated mechanical flux evaluated earlier in (2.50) as

$$L_{\mathrm{mech}}=\Gamma\sigma/2. \tag{4.25}$$

Since L_{mech} is positive, the torque has always the same sign as σ; it acts therefore to synchronize the rotation with the orbital motion.

Let us apply these results to a rotating star by treating σ as the apparent frequency of the tide, $\sigma=2(\omega-\Omega)$, where Ω and ω are the rotational and orbital angular velocities. Under those conditions, the variation of the rotational velocity is given by

$$I\frac{d\Omega}{dt}=\Gamma, \tag{4.26}$$

© European Southern Observatory • Provided by the NASA Astrophysics Data System

1975A&A....41..329Z

I being the momentum of inertia of the star. We can usually neglect the variation of ω due to the transfer of angular momentum from the rotation to the orbital motion, which is in general small compared to that of Ω. Thus we find that the relative deviation from synchronism varies with time according to

$$\frac{d}{dt}|(\Omega-\omega)/\omega|^{-5/3}=p(s)/t_{\rm syn}\,, \tag{4.27}$$

the characteristic synchronization time being

$$1/t_{\rm syn}=5\,2^{5/3}(g_s/R)^{1/2}(MR^2/I)q^2(1+q)^{5/6}E_2(R/D)^{17/2}\,. \tag{4.28}$$

Numerical values of E_2 and I/MR^2 are given in Table 1.

In a close enough binary, this synchronization time can be substantially shorter than the lifetime of the components on the main sequence. To illustrate this, consider a system of two stars, of $10\,M_\odot$ each, with a fractional separation $R/D=0.2$, corresponding to a period of 2.02 days. The synchronization time predicted by Eq. (4.28) is $t_{\rm syn}=3.1\,10^5$ years, whereas the nuclear time is about $2\,10^7$ years. It is true that the synchronization time increases very rapidly with the separation; in this example, the synchronization time would just equal the nuclear time for $R/D=0.122$, the period then being 4.21 days.

The only likely competing mechanism to achieve synchronism is due to the equilibrium tide damped by the turbulent viscosity of the convective core, but it is much less effective. In the above example of two $10\,M_\odot$ stars separated by $R/D=0.2$, the synchronization time of that mechanism would be of the order of 10^8 years, thus exceeding the nuclear life span (Zahn, 1966).

The dynamical tide with radiative dissipation therefore appears to be the most efficient process for synchronizing close binaries, when the stars do not have a large outer convective zone. On the other hand, if the stars do have such a convection zone, then it is the equilibrium tide which causes the primary torquing, and synchronization can again be achieved in a time which is much shorter than the nuclear lifetime (Zahn, 1966).

The role of these tides will be analyzed more thoroughly in a separate paper, where we will discuss in detail how these two different mechanisms may explain the dynamical evolution of close binary stars.

5. Conclusion

We should first emphasize again that the results presented here are strictly valid only for non-rotating stars. It would be highly desirable to extend this non-adiabatic analysis to rotating stars, but to do so is not a trivial matter. We should point out that even the adiabatic oscillations have yet to be studied in rotating stars when the pulsational and rotational periods are of the same order.

One purpose of this work was to clear up the curious behavior we previously reported (Zahn, 1970) for the forced oscillation near the surface of a star, when the pulsation is assumed to be adiabatic. The present study shows that such large-amplitude surface response is no longer present when radiative dissipation is taken in account. We find here that as the period increases (for a fixed excitation potential), the resonances become more and more damped and that the surface amplitude eventually decreases.

But the most interesting results bear on the oscillations excited in a star which is a member of a close binary system. Due to radiative dissipation near the surface of the star, these dynamical tidal oscillations do not have the same symmetry properties as the exciting potential. We have described here the two principal observable consequences of this lack of symmetry:

i) A torque is applied to the star, which tends to synchronize its rotation with the orbital motion. This torque is strong enough in relatively close binary systems to achieve synchronization in a time which is short compared to the nuclear lifetime.

ii) At times when the rotation of a binary component still departs significantly from synchronism, the brightness distribution over this star's surface is generally shifted with respect to the companion, thus modifying both the luminosity and the radial velocity that would be observed.

These consequences of the tides will be discussed in more detail in two subsequent papers.

Acknowledgements. I wish to thank J. Toomre for his very helpful comments on the manuscript, and M. Aizenman for kindly providing the stellar models used here in the numerical calculations. This work has been completed while I was at the Joint Institute for Laboratory Astrophysics, as a Visiting Fellow.

References

Aizenman, M. 1974 (private communication)
Baker, N. 1966, Stellar Evolution, Stein and Cameron, edit., Plenum Press, New York, 333
Baker, N., Kippenhahn, R. 1962, *Z. Astrophys.* **54**, 114
Burlisch, R., Stoer, J. 1966, *Numer. Math.* **8**, 1
Cowling, T. G. 1941, *Monthly Notices Roy. Astron. Soc.* **101**, 367
Cowling, T. G., Newing, R. A. 1949, *Astrophys. J.* **109**, 367
Hénon, M. 1967 (private communication)
Ledoux, P. 1951, *Astrophys. J.* **114**, 373
Okamoto, I., Unno, W. 1967, *Publ. Astron. Soc. Japan* **19**, 154
Plavec, M. 1970, Stellar Rotation, Slettebak, edit., Reidel Publ., Co., 133
Zahn, J.-P. 1966, *Ann. Astrophys.* **29**, 313, 489 and 565
Zahn, J.-P. 1970, *Astron. & Astrophys.* **4**, 452

J.-P. Zahn
Observatoire de Nice
F-06300 Nice

© European Southern Observatory • Provided by the NASA Astrophysics Data System